Journal of Information Systems Engineering and Management
2025, 10(40s)
e-ISSN: 2468-4376
https://www.jisem-journal.com/

Research Article

Identification and Classification of Acute Lymphocytic Leukemia Using Weighted Ensemble Neural Networks

Hema Patel[1*], Atul Patel[1], Gayatri Patel[2], Himal Shah[3]
[1] *Smt. Chandaben Mohanbhai Patel Institute of Computer Applications, Charotar University of Science and Technology, CHARUSAT – Campus, Changa – 388421, Anand, Gujarat, India*
[2] *Ramanbhai Patel College of Pharmacy, Charotar University of Science and Technology, CHARUSAT – Campus, Changa – 388421, Anand, Gujarat, India*
[3] *QURE Haematology Centre, Ahmedabad –380006, Gujarat, India*
Corresponding Author: Hema Patel
Assistant Professor Faculty of Computer Applications Smt. Chandaben Mohanbhai Patel Institute of Computer Applications, Charotar University of Science and Technology Email: hemapatel.mca@charusat.ac.in
https://orcid.org/0009-0004-2123-353X Cell: +91 9978217755

ARTICLE INFO

Received: 29 Dec 2024
Revised: 12 Feb 2025
Accepted: 27 Feb 2025

ABSTRACT

Hematologic malignancy puts the lives of numerous people of all the ages at serious risk globally. Acute lymphoblastic leukemia (ALL), a sub type of leukemia, is a dreadful disease that affects millions of individual globally. Early detection is crucial, and image analysis of peripheral blood smears is a simple way to diagnose and categorize leukemic cells. However, image analysis is complex and can lead to incorrect findings. To address this, a model is proposed to examine ALL and identify its various categories using deep ensemble learning. This study shows that a deep learning method based on an ensemble weight threshold improves leukemia detection using imbalanced dataset which reflects the real-life scenario. The proposed model examines healthy and ALL cells and identify its various categories, including Benign, Pro-B, Early Pre-B, and Pre-B from peripheral blood smear images to help in the early detection of this life-threatening disease with the highest accuracy (99.96%), precision (99.86%), sensitivity (99.93%), specificity (99.97%), F1-Score (99.89%). The model also outperforms five other pre-trained networks, viz. AlexNet, VGG-16, DenseNet-210, ResNet-50, and MobileNetV2 in classification accuracy, demonstrating its potential as an effective early diagnostic tool for ALL and its subtypes.

Keywords: Diagnosis, deep learning, leukemia, classification, ensemble neural network.

1. INTRODUCTION

Leukemia, a blood ailment triggered by bone marrow impairment, can be diagnosed manually or through conventional methods, though these approaches are time-consuming and prone to errors due to fatigue, camera quality, and pathologist experience. To address these limitations, artificial intelligence (AI)-based digital microscopic examination of blood smear images has emerged as a faster, cost-effective, and more reliable alternative [1][2]. Bone marrow, responsible for blood production, comprises white blood cells (WBCs), red blood cells (RBCs), and platelets. While RBCs transport oxygen, WBCs (or leukocytes) defend the body against infections, with deficiencies in leukocyte production leading to leukemia. WBCs are categorized into granulocytes (eosinophils, basophils, neutrophils) and agranulocytes (lymphocytes, monocytes) [2][3][4]. Leukemia is classified based on the affected leukocyte type, with lymphoblastic leukemia arising from lymphocyte abnormalities and myeloid leukemia from monocyte anomalies. Depending on disease progression, leukemia is classified into Acute Lymphocytic Leukemia (ALL), Acute Myeloid Leukemia (AML), Chronic Lymphocytic Leukemia (CLL), and Chronic Myeloid Leukemia (CML). ALL, the most common pediatric leukemia [5], further subdivides into B-cell ALL (B-ALL), affecting children aged 1–5 years and being more prevalent but less severe than T-cell ALL; T-cell ALL, primarily impacting adults over 50; and the rare NK-cell ALL, involving abnormal natural killer cell proliferation [6][7][8]. B-cell ALL, the most frequent subtype, involves abnormal B-cell development across different stages, ranging from hematopoietic stem cells to mature B-cells, including Pro-B, Early Pre-B, Pre-B, and immature B-cells, as shown in Fig 1. Traditional diagnostic methods

Journal of Information Systems Engineering and Management
2025, 10(40s)
e-ISSN: 2468-4376
https://www.jisem-journal.com/

Research Article

face challenges, including inconsistent results among physicians, misidentification due to fatigue or illness, prolonged evaluation time, and high laboratory test costs. AI-based techniques mitigate these limitations, enhancing diagnostic accuracy and efficiency.

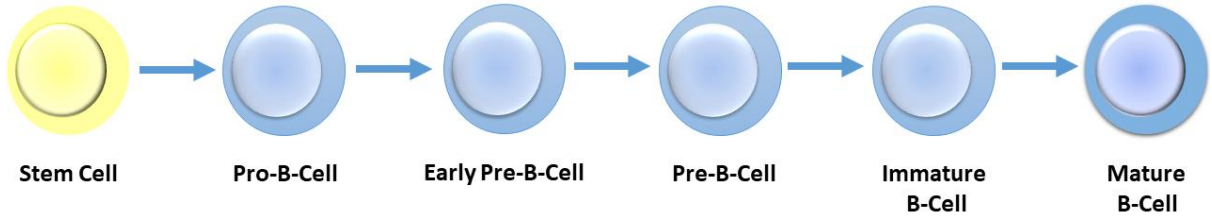

Fig 1. Stages of B-Cell Development

To address challenges in manual peripheral blood smear (PBS) examination, researchers have shifted towards automated computer-aided leukemia detection using Machine Learning (ML) procedures, which rely on the hand-crafted features for classification [9]. However, ML-based methods struggle with multi-dimensional data, dimensionality reduction, and feature extraction. Deep Learning (DL) techniques offer a robust solution by automatically identifying relevant features from large datasets and extracting deep representations from input images [10].

The primary objective is to develop a system to detect leukaemia at an early stage through blood smear images through the application of an Ensemble Neural Network.

Using the selected ALL dataset, we have tested and compared the performance of five pre-trained networks for varying input images resolutions with the imbalanced dataset in this research. The following are the key elements of our contributions:

- Proposed model is developed by performing ensemble of CNN models viz., DenseNet -121, and ResNet50, for detection and classification of healthy and malignant cells.
- The proposed weighted ensemble model, which is fine tuned, incorporates several pre-processing phases such as data resizing, balancing and augmentation.
- Data augmentation lessens data overfitting challenges, raises the generalization capacity of the model, and ultimately enhances the forecasting ability of the proposed weighted ensemble fine-tuned model.
- The technique of random oversampling has been used to alleviate the issue of class imbalance for training.
- The weighted ensemble models' outputs have been computed and gathered using a threshold, ensuring the appropriate outcomes.
- Detect and correct the mistakenly processed images by individual network. False negative images were corrected into true positive and false positive images were corrected into true negative images and stored in the separated folders.
- The suggested model has been compared with other five pre-trained networks viz., AlexNet, ResNet-50, DensNet-201, VGGNet-16, and MobileNetV2 using the selected dataset with different size of input images. This comparison study also showed that the suggested approach works superior in identifying ALL and its subtypes.

There are six sections in this study, each of which focusses on a distinct research field. In Section 2, the several ML and DL methods used to distinguish between acute and chronic leukaemia are explained in detail. An overview of the proposed system's architecture is provided in Section 3. Section 4 offers a succinct overview of the model, while Section 5 discusses the tests and findings, and Section 6 offers the future scope and conclusion.

2. LITERATURE REVIEW

With regard to computer-aided cancer detection for a variety of cancer types, DL algorithms have produced encouraging results. The promise of DL in identifying malignant cells is demonstrated by the following recent research publications.

Journal of Information Systems Engineering and Management
2025, 10(40s)
e-ISSN: 2468-4376
https://www.jisem-journal.com/

Research Article

Image segmentation process was accomplished by entropy-based hybrid model. From there, statistical and image-level information were taken out of each segment. Subsequently, the leukaemia was detected by applying the chosen features to the suggested classifier on the ALL-IDB2 database by Jha et al. [11]. Marzahl et al. [12] has designed a DL-based architecture by utilizing two augmentation methods and a normalization-based pre-processing phase. To anticipate the bounding box for classification, researchers used the ResNet18 model in conjunction with an extra regression head. WBC image characteristics were recovered by Vogado et al. [13] using three distinct CNN architectures, namely, AlexNet, VGG-f, and CaffeNet. The authors then utilized a gain ratio technique to determine features, which is used to identify key information and pertinent qualities. Ultimately, they decided to use an SVM classifier to categorize the features they had chosen. Rezayi et al. [14] utilized two networks: VGG-16 and ResNet-50. To categorize acute lymphoblastic leukemia into two groups: healthy and cancerous, a neural network of ten convolutional layers and two ∗ max-pooling layers—with strides 2—was proposed. Six standard ML algorithms were created.

In order to identify ALL from microscopic smear images, Atteia et al. [15] suggested an optimum Bayesian CNN that was trained using a hybrid dataset, improving performance through data augmentation. A hybrid dataset was created by combining two publically available datasets in order to train and assess the proposed Bayesian optimum CNN. An automated stain-normalized WBC classifier that can distinguish between normal and cancerous cells was created by Kulhalli et al. [16]. Authors demonstrated that the ResNeXt versions worked well when using the same ensemble technique as the ResNeXt-50 and ResNetXt-101 network. Park et al. [17] proposed a DL-based model that would categorise blood smear images of 12 distinct cell types with EfficientNet-V2 (B2) model. Bibi et al. [18] proposed a paradigm for identifying different types of leukemia, including CLL, CML, ALL, AML, and healthy cells, using blood smear images from the ALL-IDB and ASH databases. They used the Internet of Medical Things (IoMT) to upload the images from an IoT-enabled microscope to a "leukemia cloud." The images were then diagnosed using ResNet-34 or DenseNet-121 models. After diagnosis, the test results were sent to the physician's computer, where they used the information to make treatment decisions based on the test report data via the IoMT framework.

Veeraiah et al. [19] introduced the integration of Principal Component Analysis (PCA) and Mayfly optimisation with Generative Adversarial Network (MayGAN) to classify leukemia types as ALL, AML, CLL, CML, and abnormal White blood cells. Similarly, Wang et al. [20], implemented two leukocyte recognition methods “Single Shot Multibox Detector and an Incremental Improvement Version of You Only Look Once”.

Jawahar et al. [21] focused on eosinophils, neutrophils, monocytes, and lymphocytes and presented the “Deep Dilated Residual Convolutional Neural Network (DDRNet)” for the categorization of blood cell pictures. For faster convergence, the model utilized Deep Residual Dilated Blocks (DRDB) to improve feature extraction and address issues like vanishing gradients. The leukemia prediction system, created by Abbasi et al. [22], uses ML and DL algorithms to accurately assess multi-omics data. This method successfully filters unstructured data, highlighting the importance of DL for leukemia prediction by including 17 distinct factors, which were age of the patient, gender, type of mutation, treatment approaches, chromosomes, etc., which were used to validate the test. In order to provide a technique for developing an image classifier that employs the idea of a convolution neural network to categorise the various stages of CML, including the chronic phase, accelerated phase, and blast crisis phase was presented by Khosla et al. [23]. Amjad Rehman et al. [24] used the deep CNN classifier AlexNet and Hue, Saturation, Value driven thresholding for image segmentation to classify ALL. Arivuselvam et al. [25] employed CNN-based DL (DCNN - ResNet-34 & DenseNet-121) as a feature extractor to aid in the classification of leukemia kinds. ASH and ALL-IDB datasets were encouraged in the research phase to distinguish between the positive and the negative images in order to validate the effectiveness of this DCNN technique.

To sum up, ML and DL techniques have demonstrated remarkable promise in the identification and categorisation of leukaemia from PBS images and may be employed as a tool to support earlier and more precise leukaemia diagnosis and classification. All of these studies achieved notable levels of accuracy despite using various methodologies and datasets.

Journal of Information Systems Engineering and Management
2025, 10(40s)
e-ISSN: 2468-4376
https://www.jisem-journal.com/

Research Article

3. METHODOLOGY

In this proposed study, identification and categorization of leukocytes into healthy, Early-B cells, Pro-B cells, and Pre-B cells with the implementation of the proposed model. The suggested model is a weighted threshold-based ensemble fine-tuned neural network which has been developed by integrating two CNN networks together in the parallel fashion, namely: DenseNet-201, and ResNet50, capable to improve the accuracy of the suggested model, which is used to classify the cells into healthy and Pro-B, Early Pre-B, and Pre-B categories using blood smear images. A block illustration of the proposed model is depicted in Fig. 2. Images of the blood smear of ALL publically available datasets are used to train our proposed model. The ensemble network analyses images of the dataset and automatically acquires the features required for image classification during training. The proposed ensemble model categorizes the cells into various classes with the advised combination of weight factor and threshold.

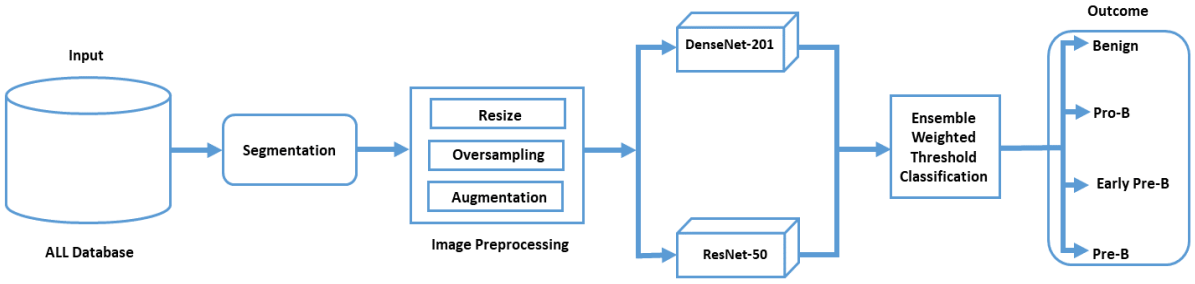

Fig. 2 Schematic Diagram of Proposed Model

3.1 Dataset

Images for the proposed system were acquired from Acute Lymphoblastic Leukemia (ALL) dataset, publically available on Kaggle databank [26]. This PBS image dataset consists of 3256 images, collected form 89 patients. Professional technicians developed and dyed the slides of blood smear images. Benign and Leukemia are the two major groups into which the dataset is divided. The benign class includes healthy cells, which are normal B-lymphocyte cells that occur spontaneously in healthy people's bone marrow and carefully resemble cases of acute lymphoblastic leukemia. On the other hand, the latter is further classified into three sub-categories of lymphoblasts, which are Pro-B, Early Pre-B, and Pre-B. Fig. 3 gives the view of randomly selected images of all the types from the dataset.

(a) Benign

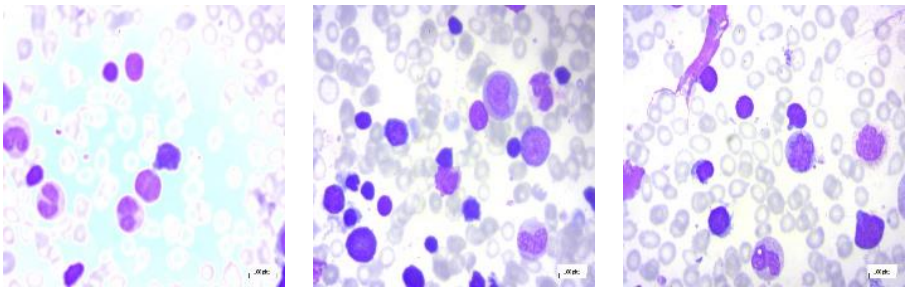

(b) Pro-B

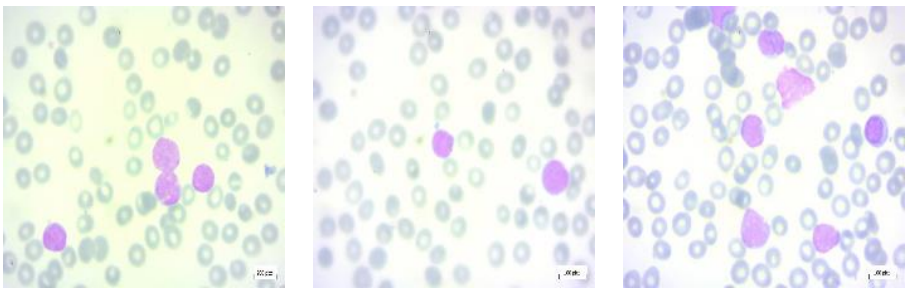

Journal of Information Systems Engineering and Management
2025, 10(40s)
e-ISSN: 2468-4376
https://www.jisem-journal.com/

Research Article

(c) Early Pre-B

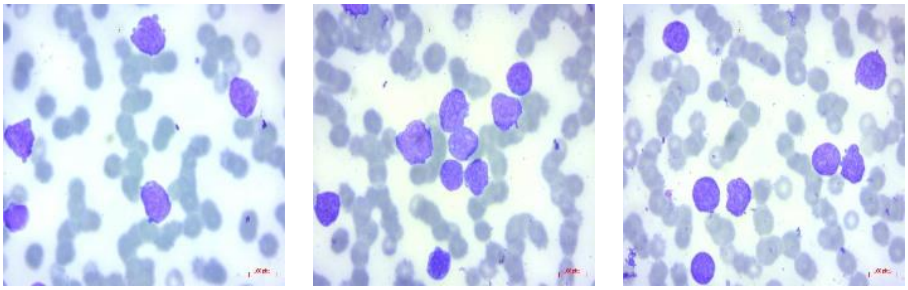

(d) Pre-B

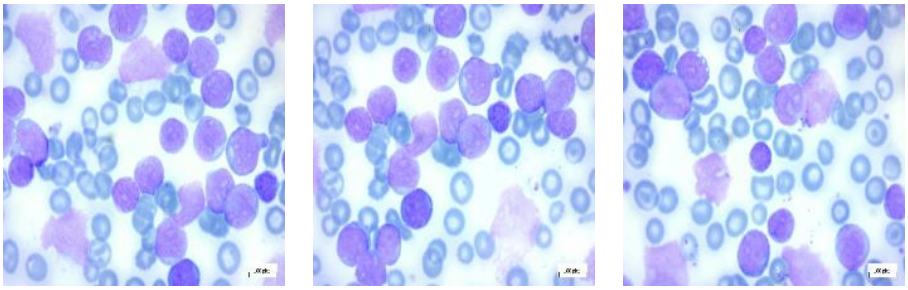

Fig. 3 Benign, Pro-B, Early Pre-B, and Pre-B

An optical microscope fitted with a Zeiss camera with a 100X amplification was used to take all of the PBS images taken from these slides, and they were all saved in JPG format. Then, using the flow cytometry technique, medical technicians classified these PBS images definitively into a certain kind and subtypes. Table 1 shows the distributing of the images among the different categories of the dataset.

Table 1. Overview of the Dataset

Type	No. of Blood Smear Images	No. of Patients
Benign	504	25
Early Pre-B	985	20
Pre-B	963	21
Pro-B	804	23
Total	**3256**	89

3.2 Segmentation

In the segmentation process, region of interest (ROI) [27] is extracted from the image. In order to successfully identify ALL instances and their corresponding subgroups, our main emphasis is on the identification of lymphoblasts, undeveloped lymphocytes. These immature lymphocytes can be retrieved from the blood smear images by employing segmentation, which defines the borders of blood cells and retrieves the vital blast cells without merging superfluous blood elements.

In our study, the ROI, lymphoblast cells, was separated from PBS images using threshold and colour interval separation methods. The practice of identifying distinct areas of an image using specific colour intensity ranges is known as colour interval separation in segmentation. It is possible to divide the image into significant areas according

Journal of Information Systems Engineering and Management
2025, 10(40s)
e-ISSN: 2468-4376
https://www.jisem-journal.com/

Research Article

to their colour characteristics by specifying threshold values and this can be easily done using HSV colour model [28] as hue element is responsible to represent the image with its original colour shades. So, our RGB colour based PSB images firstly converted into HSV space. Then, two upper and lower thresholds were defined for these images, which was finally followed by the application of binary mask to fulfil the purpose of extracting the lymphoblasts efficiently.

3.3 Preprocessing

The most common and yet most important technique for preparing input data in computer-aided applications is preprocessing, which has a direct effect on how well DL models anticipate outcomes by eliminating noise, highlighting essential features of the images [29]. For this study, three phases have been used to process the data, namely, resizing of data, data normalization, balancing of dataset and augmentation.

3.3.1 Data Resize

In order to preserve network architecture adaptability and minimize computing load, input images in convolutional networks are frequently resized. In this study, we have resized the input images as per the requirement of the different architectures (227 × 227 × 3 in AlexNet, and 224 × 224 × 3 pixels for rest of the architectures). The recommended image size for the proposed model is 224 × 224 × 3 pixels balances computational effectiveness and the accuracy of the model.

3.3.2 Balanced Classes

A common issue in DL is imbalanced classes, in which datasets have an uneven distribution of images among the different classes and it is quite usual in medical domain. To deal with this issue, we need to use the balanced classes (classes with similar no. of images) because training the model using imbalanced data may result in erroneous outcome and impair the learning model's functionality. The dataset in our research has imbalanced classes with least no. of images in Benign class (minority class). To solve this problem, we have utilised random oversampling technique [30]. In this technique, images are randomly chosen from the minority class and duplicated and added to the training data to balance the unbalanced class. For testing, we utilized the original imbalanced dataset, as it closely resembles real-life scenarios.

3.3.3 Data Augmentation

Data augmentation is one of the well-known procedure thorough which images can be altered by translating and rotating etc. [31]. This guarantees keeping useful facts intact while addressing data overfitting issues, which in turn enhances the system's overall performance. In this research, we have incorporated some augmentation techniques, including random rotation in both directions by providing positive and negative values, horizontal and vertical translation of images, and random scaling of images along the X-axis and Y-axis. In this way, we may artificially extend the variation of the training dataset, which assists to strengthen the resilience and adaptability of DL networks.

3.4 Convolutional Neural Networks / Classifier

One kind of artificial neural network that is utilised for processing and image identification is the convolutional neural network (CNN) [32]. Identifying patterns in images is a significant application of CNNs. So, it can be said that CNNs can be thought of as a classifier which is made up of numerous layers which may vary from network to network.

3.4.1 DenseNet-201

The goal of the deep neural network architecture DenseNet-201 (Densely Connected Convolutional Network) is to increase model efficiency overall, feature reuse, and gradient flow. It is an expansion of the original DenseNet architecture, which has 201 layers with feed-forward connections between each layer [33]. DenseNet-201 guarantees that all previous layers contribute to the feature maps of the current layer, improving information transmission and minimizing duplicated computations, in contrast to conventional convolutional networks where each layer only receives input from the previous layer. Comparing this structure to architectures like ResNet, the vanishing gradient issue is greatly reduced, and the model may learn more discriminative and detailed features with less parameters. In order to maximize computational efficiency and minimize feature map dimensions without compromising speed, DenseNet-201 also uses bottleneck and transition layers. A popular option for leukemia detection and classification

Journal of Information Systems Engineering and Management
2025, 10(40s)
e-ISSN: 2468-4376
https://www.jisem-journal.com/

Research Article

in blood smear images, DenseNet-201 is used extensively in medical imaging, object recognition, and fine-grained classification applications because of its capacity to grasp complex spatial hierarchies in images.

3.4.2 ResNet-50

ResNet-50 belongs to ResNet series, which was developed by Kaiming He and associates in the year 2015. With 50 layers, the ResNet-50 neural network can reveal complicated and hidden associations from the data it receives. The primary component of ResNet-50 is the residual building blocks (RBB) [34], which optimize the training of deep neural networks and address the issue of vanishing gradients by implementing the shortcut or skip connections. In order to avoid vanishing gradients, these connections avoid one or more layers and permit the gradient to run across the network during the process of backpropagation. As a result, this model performs extremely well on a variety of applications involving computer vision and serves as a preferred solution for transfer learning in numerous areas for instance, image classification, medical imaging, object detection etc.

There are 4 residual blocks which is preceded by convolutional layer. Other layers are batch normalization, then a ReLU activation function which is eventually followed by a fully connected layer. Here, "50" stands for the total number of weight layers, including convolutional and fully connected layers. So, if we use the preceding weight layer as the procedure of feature engineering, local feature extraction and local amplification [35], the last FC layer can be assumed as a feature weighting layer [36].

Shortcut connection is introduced by Resnet-50 which is also known as shortcut connections. To understand this, the two distinct RBB structures are depicted with the help of Fig. 6. Here, three convolutional and BN layers are present in both the structures. The identity x is used to denote the shortcut connection in Fig. 4 (a) [34] and the outcome of this can be expressed using Eq. 1 [34], where F represents the nonlinear function, which is used for the convolutional path in the structure A. The structure's B construction is shown in Fig. 6 (b) [34]. There is one alternate of convolutional and BN layers and the result of this structure can be defined by Eq. 2 [34], where H represents the shortcut path.

$$Y = F(x) + x \quad (1)$$

$$Y = F(x) + H(x) \quad (2)$$

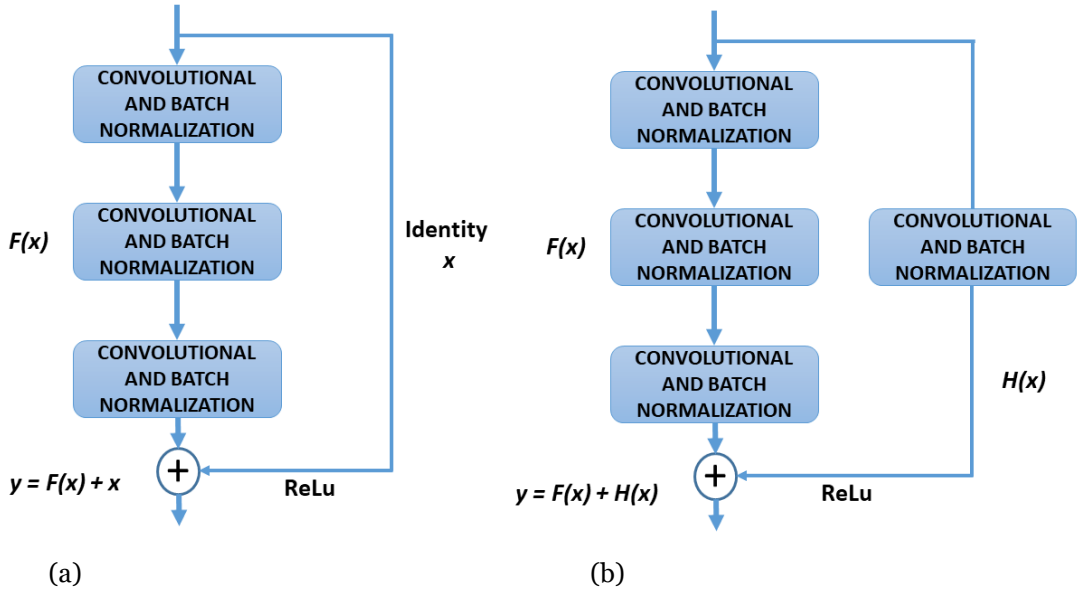

(a) (b)

Fig. 4 Structure of Residual Connections

3.4.3 AlexNet

AlexNet architecture acquired the 2012 "ImageNet Large Scale Visual Recognition Challenge (ILSVRC)". "Alex Krizhevsky, Ilya Sutskever, and Geoffrey Hinton" created it, and it brought forth important breakthroughs in DL for

Journal of Information Systems Engineering and Management
2025, 10(40s)
e-ISSN: 2468-4376
https://www.jisem-journal.com/

Research Article

image classification. Five convolutional layers along with three fully linked layers make up AlexNet's eight layers [37]. To speed up training and avoid vanishing gradients, it uses ReLU (Rectified Linear Unit) activation functions. It also uses dropout layers to keep overfitting at bay and max pooling to minimize spatial dimensions while keeping key characteristics. By employing overlapping pooling and data augmentation, the model's capacity for generalization was greatly enhanced. As the first CNN to use GPU acceleration, AlexNet showed how effective deep networks can be at tackling challenging image classification jobs. Its popularity established the groundwork for contemporary DL architectures and its continued use in a number of applications, such as feature extraction, object recognition, and medical picture analysis.

3.4.4 VGG-16

The Visual Geometry Group (VGG) unveiled VGGNet-16, one of the variant of VGGNet, renowned for its straightforward design, in the year 2014. Smaller filter sizes and deeper network topologies were used in its construction to enhance the effectiveness of CNN on classification of images.

VGG-16 comprises of total sixteen layers which includes thirteen convolutional layers, along with five max pooling layers, then three fully connected layers and at last a softmax layer for the classification. The purpose of using maximum pooling layer is to decrease the spatial size following each set of two or three convolutional layers which helps in faster generation of results.

In VGG-16, the input layer, accepts the images with the dimensions of 224 × 224 × 3. The input is subsequently sent through a number of convolutional layers, each of which applies a number of filters. To provide non-linearity to the network, the outcome of every convolutional layer is subsequently processed through an activation function called a rectified linear unit (ReLU) [38].

In order to decrease the spatial dimensions of the feature maps, VGG-16 employs max-pooling layers following a sequence of convolutional layers. Every time the feature map is applied, its size is cut in half thanks to the usual pooling size of 2x2 with a stride of 2. This downsampling strategy makes the network more efficient while maintaining key features, which helps to reduce computational time and avoid overfitting. In order to make the network resilient to spatial alterations to input images, pooling layers lower the variance of translations. Ultimately, fully connected layers that carry out the final classification process receive the outcome from the last pooling layer. Although the model is large and requires a lot of computation, it performs remarkably well in image classification.

Fig. 5 depicts the architecture of VGG-16 network. Here, convolutional layer follows the input layer, which is responsible to for the generation of the output feature maps by organizing the input image or feature map with a collection of numerous filters.

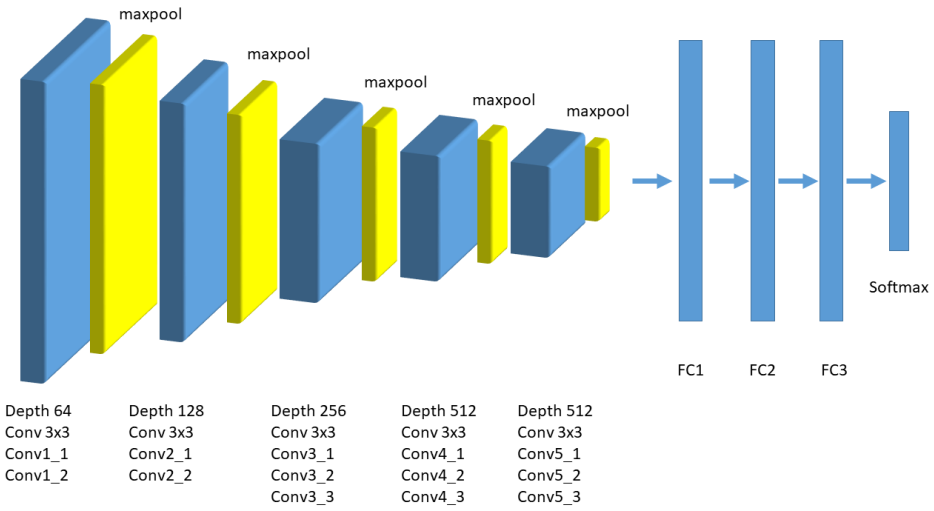

Fig. 5 Architecture of VGG-16

Journal of Information Systems Engineering and Management
2025, 10(40s)
e-ISSN: 2468-4376
https://www.jisem-journal.com/

Research Article

The input image is filtered by the initial convolutional layer in VGG-16 using a 3 × 3 filter with a stride of 1 and 1 padding with 3 no. of input channels. This can be expressed mathematically by Eq. 3:

$$O(x, y, k) = \sum_{i=1}^{3} \sum_{j=1}^{3} \sum_{c=1}^{3} I(x + i - 2, y + j - 2, c).W(i, j, c, k) + b_1 \quad (3)$$

Here, I denotes the input image or feature map with the size (H × W × C), W is the weight of the filter and b_1 indicates bias term for the filter 1.

Following every convolution, an activation function known as a ReLU (Rectified Linear Unit) is applied, as shown in Eq. 4:

$$f(x) = \max(0, x) \quad (4)$$

where the convolution operation's output is denoted by x.

For down sampling, max-pooling is employed. Mathematical equation for the polling window size 2 x 2 and stride 2 can be computed by Eq. 5:

$$P(x,y) = \max_{i=0}^{1} \max_{j=0}^{1} I(2x+i, 2y+j) \quad (5)$$

The objective of using a fully connected layer is to implement matrix-vector multiplication, as shown in Eq. 6:

$$O = W \,.\, I + b \quad (6)$$

Here, O is the resultant vector whereas I represents input vector, W symbolizes the weight matrix, and b shows bias term.

Softmax layer is employed to execute the final classification, as given in Eq. 7:

$$P(Y_i|x) = \frac{e^{z_i}}{\sum_{j=1}^{n} e^{z_i}} \quad (7)$$

Here, n represents the total number of classes whereas output from the last fully connected layer for a particular class i can be denoted by z_i.

3.4.5 MobileNetV2

A neural network architecture called MobileNet was unveiled by Google and operates incredibly well on mobile smartphones and other low-processing-power devices. In order to achieve great accuracy with the fewest possible parameters and mathematical procedures, MobileNet was developed. Inverted residual blocks and linear bottleneck layers are two significant improvements that it proposed to build on MobileNet's success. The inverted residual block enhances the feature dimension after compressing features with a small bottleneck layer and then performing a lightweight depthwise convolution.

MobileNetV1 has been enhanced to become MobileNetV2 [39]. Instead of using standard convolutional layers, which play vital role for computer vision applications but extremely expensive for computing, the MobileNetV2 architecture employs depthwise separable convolutions. The new depthwise separable convolution block comprises of three layers [40]. A 1x1 convolution layer is used as the initial layer to boost the number of channels in the input feature map before going into the depthwise convolution layer. The second layer, a 3x3 depthwise convolution layer, then filters the input feature map, and a 1x1 convolution layer comes last [41]. To reduce the quantity of channels in the input feature map, the last convolution layer projects data with a huge number of channels into a tensor by using a significantly lesser number of channels. As it lowers the volume of data that passes through the network, the last layer is also known as a bottleneck layer [42].

Journal of Information Systems Engineering and Management
2025, 10(40s)
e-ISSN: 2468-4376
https://www.jisem-journal.com/

Research Article

3.5 Ensemble Transfer Learning

Ensemble transfer learning enhances the overall performance in a specific assignment by incorporating the benefits of several already trained models into a single framework while avoiding their particular limitations. To provide a more trustworthy and authentic prediction model, it makes use of the numerous attributes that have already been learned by various architectures.

Several DL techniques have gained popularity in recent years, as seen by the research on automatic identification of ALL from microscopic analysis of blood smear images cited above. Despite the substantial amount of previously published material, a more thorough and extended model that enhances performance is still possible. Additionally, DL-based methods struggle with the lack of data to avoid model overfitting issue, the ensemble of many DL network topologies mitigates this drawback. Although there are numerous articles that use the ensemble learning method, the weighted ensemble network with threshold factor-based learning approach has not been implemented to this particular dataset or in the context of acute lymphoblastic leukemia (ALL).

In this research, our model has been developed by ensemble three well known DL networks viz. DenseNet-20, and ResNet-50 to detect healthy and cancerous cells and classify them (Healthy, Pro-B, Early Pre-B and Pre-B cells). Also, the five most frequently used pre-trained networks have been analyzed viz. AlexNet, DenseNet-210, VGGNet-16, ResNet-50, MobileNetV2. After thorough analysis, we found, our fine-tuned proposed model outperforms all these pre-trained networks as its more profound design allow it to efficiently extract complex features and characteristics from the images. Notably, the equilibrium between computing time, performance, and complexity was considered during the decision-making procedure.

3.6 Weighted Threshold-Based Ensemble Networks

Weighted threshold-based ensemble networks are widely used in various areas where high predictive accuracy is essential. Multiple models contribute to the final prediction using a weighted threshold ensemble network, an ensemble learning technique, with differing degrees of contribution depending on the weights supplied to each model. This method involves multiplying the forecast of each model by a weight that indicates its ability to perform, and then merging the weighted results. The overall result is subjected to a threshold in order to reach a conclusion. The final prediction with various weights applied on numerous DL networks can be calculated using below given Eq. 8:

$$EP = argmax(\sum_{i=1}^{n} w_i \, . p_i) \quad (8)$$

Where, n represents the total number of networks, w denotes the selected weight and p shows the prediction of the networks.

The proposed strategy has been developed by applying the concept of a heterogeneous ensemble model procedure [43]. This technique allows data to be supplied to each base framework simultaneously, for averaging out the individual errors generated by each base network efficiently. In addition, weights for every framework with a predetermined threshold have been implemented in the ensemble model. Weighted accuracy helps to address imbalanced datasets issues whereas introduction of threshold enhances the classification accuracy by diminishing misclassification errors.

3.7 Training Policy

The CNNs are widely used networks across the globe for image classification. To configure our model, we have merged three DL models, and each model consists of numerous layers. The input layer is the first one that picks up the PBS images from the dataset, which is liable to decide the size of the image. For our model, we have selected the images of the size 224 x 224 x 3, where 3 shows the number of colour channels. Which was followed by balancing the unbalanced classes and then the balanced dataset was randomly split into the proportions of 65% to the training set, and 35% to the testing set. Afterwards, two fine-tuned ensemble networks have been used in this research to enhance the performance of our model. This approach improves model accuracy while utilizing cutting-edge DL models in our investigation.

Journal of Information Systems Engineering and Management
2025, 10(40s)
e-ISSN: 2468-4376
https://www.jisem-journal.com/

Research Article

Weights in a weighted threshold-based ensemble network indicate how important or dependable each model is in influencing the final forecast. Therefore, with the help of these particular weights and threshold, the ensemble network efficiently reduces the shortcomings of each model while consolidating its strengths, improving prediction accuracy. Various weight-sets ([0.5, 0.5], [0.6, 0.4], [0.4, 0.6], [0.3, 0.7], [0.7, 0.3]) were chosen for DenseNet-201, and ResNet-50 respectively, with two different threshold factors of 0.7 and 0.8, in order to boost the efficiency of our model. As the model with the weight set 0.5, 0.5, each individual network accounts for 50% of the ensemble's eventual selection and weight set 0.7, 0.3 implies that the most accurate model during training procedure is DenseNet-201. When compared to DenseNet-201, ResNet-50 model's 30% input to the ensemble's ultimate choice suggests medium reliability. The predetermined values for the threshold factor is used to calculate the final class prediction based on the sum of the scores from the model. When a threshold of 0.7 is applied in our model, a confident classification into a certain category needs the total weighted prediction score to be greater than 70%. The appropriate class is predicted by the ensemble if threshold is greater than or equal to 0.7. Otherwise, either no confident prediction is returned or a different class is predicted. The model follows the same procedure for 0.8 value for the threshold.

An estimation optimizer, Adaptive Moment (ADAM), was also included in the final output layer and regulates the rapidly the learning rates for each parameter according to estimations of the first and second moments of gradients and it works well with noisy gradient models and huge datasets. The initial learning rate chosen for this study was 0.0001, used to handle the step size while training the dataset. A model may occasionally become stuck on its saddle points or nearby minima as a result of a monotonic decrease in the learning rate. One epoch is the process by which the training algorithm runs over the entire training dataset using numerous mini blocks of images. To train the model, we have used 10 epochs, as fewer epochs generate results quickly and aids in managing the data overfitting issues. With 10 epochs, the size of mini-batches was kept at 32, which can process 32 images in every single iteration of the entire training procedure.

When training DL models, a loss function is essential as it gauges how well the model forecasts the actual labels. In our study, Cross-Entropy Loss function is implemented to calculate how much the true label distribution differs from the predicted label distribution. This can be computed using Eq. 9:

$$L = \sum_{i=1}^{N} y_i \log(\hat{y}_i) \qquad (9)$$

Where, N denotes the total number of classes, y_i shows the actual label and $\hat{y}_i$ is the class ‘s predicted probability. Predictions that deviate significantly from the true labels are penalised by this loss function, which incentivises the network to provide increasingly precise predictions over time.

3.8 Hardware Specification

A high-performance AI supercomputer, the "4 × NVIDIA DGX Station with four NVIDIA A100 Tensor Core GPUs and 40GB of RAM each," has been used to execute the model. The proposed model is implemented using the software MATLAB 2024a. To guarantee the efficacy and equity of the comparative study, each of the methods is implemented in an identical environment.

4. EMPIRICAL ANALYSIS AND RESULTS

In this paper, we have discussed the diagnosis of healthy or malignant cells, using fine-tuned, weighted ensemble, transfer learning technique with the threshold values of 0.7 and 0.8. The proposed solution has been evaluated on the imbalanced original testing set with the objective of meeting up with the real-life scenarios. This section demonstrates the superiority of the suggested ALL categorization approach. Its performance is also contrasted with other individual DL networks, viz., AlexNet, DenseNet-201, VGGNet-16, ResNet-50 and MobileNetV2. xx A division of dataset is made as follows: 65% training data, and 35% for testing data, and 10% validation data. The proposed model outperforms in terms of accuracy when compared to other current approaches as shown in Table 2.

Journal of Information Systems Engineering and Management
2025, 10(40s)
e-ISSN: 2468-4376
https://www.jisem-journal.com/

Research Article

Table 2. Deep learning techniques for ALL classification

Sr. No.	Year	Author & References	Dataset	Data Volume	Methods	Accuracy
1.	2021	Das et al. [9]	ALLIDB1, ALLIDB2	108, 260	ResNet18 and MobilenetV2	99.39%, 97.18%
2.	2021	Kulhalli et al. [44]	C-NMC	-	Different variants of ResNeXt	85.70%
3.	2021	Genovese et al. [45]	ALL-IDB2	260	HistoTNet	97.92%
4.	2021	Putri et al. [46]	Cancer Imaging Archives	12528	ResNet-50	81.12%
5.	2022	Rezayi et al. [47]	CodaLab competition	12528	Proposed CNN	85.79%
6.	2022	Park et al. [48]	-	42,386	EfficientNet-V2 (B2)	87.79%
7.	2023	Rani et al. [49]	ASH		ResNet-50	94.12%
8.		Proposed Model	ALL	3256	DenseNet-201, ResNet-50	99.96%

In order to achieve outstanding performance and make the system computationally efficient, the threshold value (γ) is crucial. Additionally, the threshold value (γ) has been modified by simulation tests to assess the accuracy of classification outcomes. We have used different threshold values such as 0.7, 0.8 for the ALL (65%, 35%), with the various weight sets ([0.5,0.5], [0.4,0.6], [0.6,0.4], [0.3,0.7], [0.7,0.3]). Tables 3 presents a comparative analysis of the suggested model's performance with other pre-trained networks. It has been observed that the suggested approach achieves highest accuracy at γ=0.7 with weight set 0.7, 0.3.

Table 3. Performance evaluation of the proposed weighted threshold-based ensemble model for with 65% training, 35% testing data.

Weights	Threshold	Network	Class	Precision (%)	Sensitivity (%)	Specificity (%)	F1-Score (%)	Accuracy (%)
		AlexNet		99.10	95.93	98.29	99.10	97.45
		VGGNet-16		95.01	99.42	89.77	97.17	96.40
		Mobile NetV2		97.65	97.94	95.45	97.80	98.07
		ResNet-50		99.42	98.55	98.86	98.98	99.21

Journal of Information Systems Engineering and Management
2025, 10(40s)
e-ISSN: 2468-4376
https://www.jisem-journal.com/

Research Article

		DenseNet-201		99.17	99.71	98.30	99.42	99.47
0.5, 0.5	γ=0.7	Proposed	Benign	96.70	100.00	99.38	98.32	99.47
			Early-B	100.00	99.42	100.00	99.71	99.82
			Pre-B	100.00	98.81	100.00	99.40	99.65
			Pro-B	100.00	100.00	100.00	100.00	100.00
			Overall	99.18	99.56	99.84	99.36	99.74
	γ=0.8	Proposed	Benign	96.17	100.00	99.27	98.05	99.39
			Early-B	100.00	99.13	100.00	99.56	99.74
			Pre-B	100.00	98.81	100.00	99.40	99.65
			Pro-B	100.00	100.00	100.00	100.00	100.00
			Overall	99.04	99.49	99.82	99.25	99.69
0.3, 0.7	γ=0.7	Proposed	Benign	96.07	100.00	99.38	98.32	99.47
			Early-B	99.71	99.13	99.87	99.42	99.65
			Pre-B	100.00	98.81	100.00	99.40	99.65
			Pro-B	100.00	100.00	100.00	100.00	100.00
			Overall	99.10	99.49	99.81	99.29	99.69
	γ=0.8	Proposed	Benign	96.17	100.00	99.27	98.05	99.39
			Early-B	100.00	99.13	100.00	99.56	99.74
			Pre-B	100.00	98.81	100.00	99.40	99.65
			Pro-B	100.00	100.00	100.00	100.00	100.00
			Overall	99.04	99.49	99.82	99.25	99.69
0.6, 0.4	γ=0.7	Proposed	Benign	97.24	100.00	99.48	98.60	99.56
			Early-B	100.00	99.42	100.00	99.71	99.82
			Pre-B	100.00	99.11	100.00	99.55	99.74
			Pro-B	100.00	100.00	100.00	100.00	100.00
			Overall	99.31	99.63	99.87	99.47	99.78
	γ=0.8	Proposed	Benign	95.14	100.00	99.07	97.51	99.21
			Early-B	100.00	98.84	100.00	99.42	99.65
			Pre-B	100.00	98.81	100.00	99.40	99.65
			Pro-B	100.00	99.64	100.00	99.82	99.91
			Overall	98.78	99.32	99.77	99.04	99.60
	γ=0.7		Benign	96.17	100.00	99.27	98.05	99.39
			Early-B	100.00	99.13	100.00	99.56	99.74

Journal of Information Systems Engineering and Management
2025, 10(40s)
e-ISSN: 2468-4376
https://www.jisem-journal.com/

Research Article

0.4, 0.6		Proposed	Pre-B	100.00	98.81	100.00	99.40	99.65
			Pro-B	100.00	100.00	100.00	100.00	100.00
			Overall	99.04	99.49	99.82	99.25	99.69
	γ=0.8	Proposed	Benign	96.17	100.00	99.27	98.05	99.39
			Early-B	100.00	99.13	100.00	99.56	99.74
			Pre-B	100.00	98.81	100.00	99.40	99.65
			Pro-B	100.00	100.00	100.00	100.00	100.00
			Overall	99.04	99.49	99.82	99.25	99.69
0.7, 0.3	γ=0.7	Proposed	Benign	99.44	100.00	99.90	99.72	99.91
			Early-B	100.00	100.00	100.00	100.00	100.00
			Pre-B	100.00	99.70	100.00	99.85	99.91
			Pro-B	100.00	100.00	100.00	100.00	100.00
			Overall	**99.86**	**99.93**	**99.97**	**99.89**	**99.96**
	γ=0.8	Proposed	Benign	96.17	100.00	99.27	98.05	99.39
			Early-B	100.00	99.13	100.00	99.56	99.74
			Pre-B	100.00	99.11	100.00	99.55	99.74
			Pro-B	100.00	99.64	100.00	99.82	99.91
			Overall	99.04	99.47	99.82	99.25	99.69

Table 3 presents the performance outcomes achieved by the proposed model for identifying and categorizing each category of the blood smear images in healthy and subtypes of cancerous cells. We can see from the tables that the proposed strategy obtained the highest accuracy (99.96%), precision (99.86%), sensitivity (99.93%), specificity (99.97%), F1 score (99.89%) when compared to other models. It can be said to perform better than the others—also, the suggested model obtained 99.91% ensemble accuracy and 0.0000 ensemble loss.

We also generated a confusion matrix to provide a pictorial overview of the outcomes derived from the test data. The accurately categorized images for each category are represented by the diagonal values. Images that have been incorrectly categorized by the model are represented by entries other than the diagonal value. Most of the images are accurately identified by our proposed model, as shown in Fig. 6. Nevertheless, it only incorrectly identifies 1 image from the Pre-B category as Benign which can be consider as the false negative. Also, model achieved 100% true positive rate for other three categories: Benign, Early-Pre-B, and Pro-B.

Journal of Information Systems Engineering and Management
2025, 10(40s)
e-ISSN: 2468-4376
https://www.jisem-journal.com/

Research Article

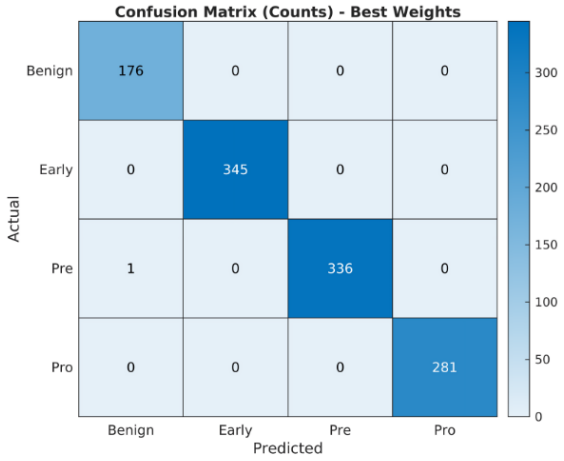

(a)

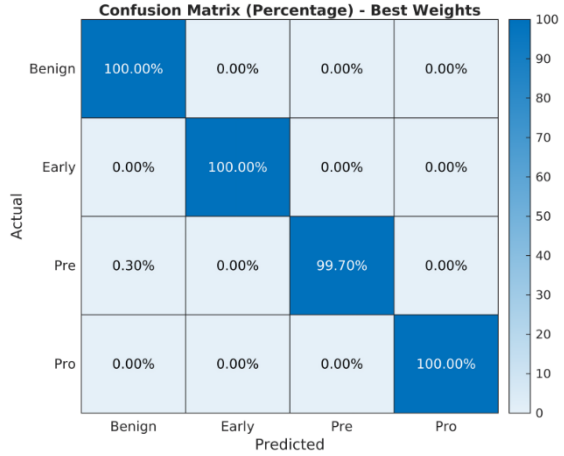

(b)

Fig. 6 Confusion Matrix, (a) Confusion Matrix (Value), (b) Confusion Matrix (Percentage)

Fig. 7 represents the curve of Receiver Operating Characteristic (ROC). The suggested approach produces the best ROC curve with 35% testing data with the best Area Under Curve (AUC) of 1.00, whereas DenseNet201 framework obtained the second-best ROC with an AUC of 0.97, and VGG-16 network achieved the least AUC of 0.93.

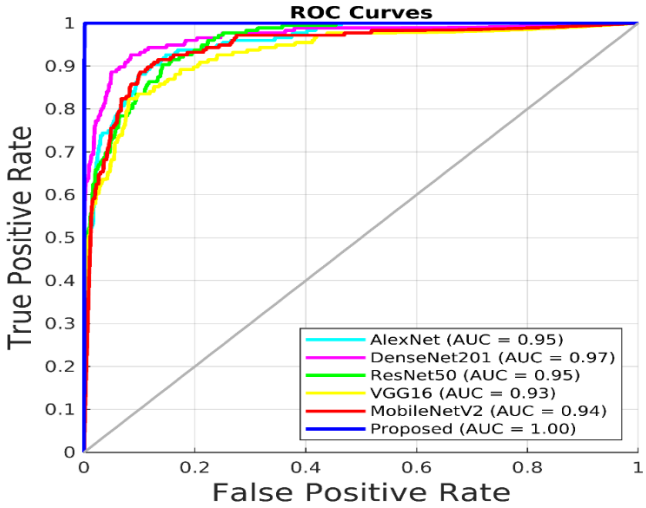

Fig. 7 ROC Curve

Journal of Information Systems Engineering and Management
2025, 10(40s)
e-ISSN: 2468-4376
https://www.jisem-journal.com/

Research Article

Overall, these results show how crucial an ideal threshold value and weight allocation are to attaining better classification results. The findings show that in addition to increasing the accuracy of leukemia identification, the suggested ensemble learning approach guarantees a trustworthy classification framework for practical medical applications. With weights [0.7, 0.3] and an improved model at γ = 0.7, the best-performing configuration achieves an almost ideal balance of precision, specificity, and sensitivity.

5. DISCUSSION

In order to increase the model's capacity for learning and boost classification performance, we trained it on a balanced and oversampled dataset. We specifically raised the training dataset's PBS image count from 2117 to 2560 to guarantee a more consistent class distribution. To prevent the model from biasing to majority classes during training, this oversampling strategy helps to deal with the issue of class imbalance. We used the original imbalanced dataset for testing; nevertheless, to replicate real-world situations in which the actual test dataset is imbalanced. In addition, performance measurements could be altered by a balanced test set, whereas an imbalanced dataset more accurately evaluates the data. This method guarantees the model's resilience and generalisability when used on actual medical datasets by enabling a more realistic assessment of its performance.

Here, we demonstrate how the threshold is necessary for the accuracy of the suggested model. In our study, several weight sets and threshold values (γ) have been used to assess the efficacy of the suggested weighted threshold-based ensemble model. Choosing the ideal threshold value is essential for both high classification accuracy and computing economy. To find the best setup for categorizing distinct leukemia subtypes, simulation tests were conducted to explore threshold values of 0.7 and 0.8 across a range of weight combinations. The model only misclassifies an instance as a non-leukemic image when the threshold has been assigned to 0.7 and the estimated probability is more than 70%. This configuration minimizes false positives while preserving excellent accuracy by ensuring an equitable balance between sensitivity and specificity.

The suggested model clearly performs better than traditional pre-trained networks like AlexNet, VGGNet-16, MobileNetV2, ResNet-50, and DenseNet-201 in terms of accuracy, precision, sensitivity, specificity, and F1-score, as shown by the findings in Table 2. In order to maximize classification performance, the suggested ensemble strategy assigns several weight distributions, combining the advantages of ResNet-50 and MobileNetV2. Regarding the final classification decision, the weight set (0.7, 0.3) in the suggested ensemble model indicates the respective contributions of the two DL architectures, DenseNet-201 and ResNet-50. DenseNet-201 influences 60% of the decision-making process in this setup, whereas ResNet-50 influences 40%.

Our proposed model obtained the overall highest accuracy of 99.96% for γ = 0.7. Since all leukemia subtypes show consistently strong classification metrics, the class-wise evaluation further supports the suggested approach's robustness. Particularly, the model demonstrates its capacity to reliably identify Early-Pre-B, Pre-B, and Pro-B leukemia subtypes by achieving 100% precision and specificity. The model's ability to distinguish between benign and malignant instances is still quite trustworthy, as seen by the small fluctuation in benign categorization (precision: 99.44%, sensitivity: 100.00%, specificity: 99.90%). But overall accuracy falls to 99.69%, indicating a modest decline in performance when the threshold is raised to γ = 0.8. This suggests that some minor incorrect classifications could occur from a more restrictive classification method brought on by a higher criterion. Because it balances the trade-off between sensitivity and specificity and maximizes classification accuracy, the weight allocation of [0.7, 0.3] at γ = 0.7 continues to be the best option.

This arrangement of threshold and weight set is also helpful in increasing the true positive rate while retaining the false positive rate lower, as depicted in Fig. 2. When the confusion matrix is calculated with 1139 PBS images of the test dataset. Out of these 1139 images, 176 images have been reserved for the Benign class, 345 for the Early-Pre-B class, 337 samples for the Pro-B class, and 281 for the Pro-B class. The model achieved a 100% true positive rate for Benign class, Early-Pre-B class, and Pro-B class which means that every case of each of these categories was correctly identified, and there were no other false positives or false negatives. One case, though, was incorrectly classified as Benign from the Pre-B category, resulting in a false negative. Notwithstanding this little error, the overall accuracy of classification is still excellent, illustrating the usefulness of the suggested weighted threshold-based ensemble

Journal of Information Systems Engineering and Management
2025, 10(40s)
e-ISSN: 2468-4376
https://www.jisem-journal.com/

Research Article

model. In continuation with this, this also helps in achieving the best ROC curve, as shown in Fig. 3, with an extraordinary Area Under the Curve (AUC) of 1.00.

The significance of our ensemble model can also be stated through its capability to recognize mistakenly classified images individually by pre-trained networks, DenseNet201 and ResNet-50. The proposed model turns false positive images into true negative images and false negative images into true positive images. If one of the individual models cannot produce an accurate prediction, another model in our ensemble model can rectify the errors and assist in mitigating the number of false positive and false negative images. The corrected images are stored in the new folders, created as per the conversion, one for false positive to true negative and another for false negative to true positive. In addition, the count of the total number of faulty images and the corrected images with the list of their names along with the path by our model also shows the proficiency of the model. As a result, we can state that our ensemble model helps us make more reliable and efficient medical decisions by yielding more accurate and correct outcomes than an individual network. Therefore, an appropriate diagnosis can increase a patient's chances of survival while lessening their economic responsibilities and psychological loads.

This model demonstrates a robust ability to differentiate between the various stages, emphasizing its potential for clinical applications in diagnostics. Furthermore, such performance metrics suggest that the model can be confidently deployed in real-world scenarios, where accuracy is paramount. Future research may focus on refining the model further to reduce instances of misclassification and enhance its applicability across larger datasets.

6. CONCLUSION AND FUTURE SCOPE

ALL is one of the severe illness which affects the children as well as elderly people. To survive against this illness, it is essential to diagnose this on the initial stage with its specific sub-type.

The manual medical practices require much time and attention for the proper identification and classification of the leukemic cell from the blood smear images. Therefore, we have proposed the model, based on ensemble weighted threshold-based technique. The suggested model recognizes healthy and malignant cells and also categorize into its sub-types as Benign, Pro-B, Early Pre-B, and Pre-B.

The model, for identifying and categorizing leukemic and healthy cells that is based on an ensemble weight threshold efficiently utilizes the advantages of two DL frameworks, such as DenseNet-201, and ResNet50. By providing the optimum weights and setting a threshold, the proposed model optimizes classification precision as well as accuracy. Also, by lowering misdiagnosis rates and boosting diagnostic exactness, the model guarantees reliable feature extraction. With the implementation of class-wise accuracy, the evaluation procedure is further improved and equitable assessment of proficiency across classes is guaranteed. The findings show that the ensemble model identifies healthy and leukemic cells and classifies leukemic cells into its sub-types more accurately than individual networks, which makes it a useful tool for automated leukemia detection and classification.

This study demonstrates how AI may significantly increase the speed and accuracy of haematological diagnostics, providing a potent tool for the early diagnosis and treatment of diseases like leukaemia. Future work may delve into improving the models even more, testing them on bigger and more varied datasets, and investigating how they might be incorporated into clinical settings. The efficacious use of CNN within this particular domain presents auspicious prospects for the automated examination of medical imagery, hence augmenting the efficiency and scalability of diagnostic procedures.

FUNDING

This research received no specific grant from public, commercial, or not-for-profit funding agencies.

CONSENT FOR PUBLICATION

Not applicable.

CONFLICT OF INTEREST

The authors declare no conflict of interest.

Journal of Information Systems Engineering and Management
2025, 10(40s)
e-ISSN: 2468-4376
https://www.jisem-journal.com/

Research Article

AUTHOR CONTRIBUTIONS

Conceptualization, material preparation, data collection, writing, and analysis were performed by the first author. Conceptualization, review & editing were performed by the second and third authors. The review was accomplished by a forth author.

ACKNOWLEDGEMENT

My profound appreciation goes out to the administration of Charotar University of Science and Technology for their constant encouragement and support during the writing of this review study.

REFERENCES

[1] Chastine Martin Leonard Tangel, Muhammad Rahmat Widyanto, Fangyan Dong, and Kaoru Hirota. "Interest-based ordering for fuzzy morphology on white blood cell image segmentation." Journal of Advanced Computational Intelligence and Intelligent Informatics 16, no. 1 (2012): 76-86.

[2] Amy Glenn, Catherine E. Armstrong, Physiology of red and white blood cells, Anaesthesia & Intensive Care Medicine, Volume 20, Issue 3, 2019, Pages 170-174, ISSN 1472-0299, https://doi.org/10.1016/j.mpaic.2019.01.001.

[3] Lorenzo Putzu, Giovanni Caocci, Cecilia Di Ruberto, Leucocyte classification for leukaemia detection using image processing techniques, Artificial Intelligence in Medicine, Volume 62, Issue 3, 2014, Pages 179-191, ISSN 0933-3657, https://doi.org/10.1016/j.artmed.2014.09.002.

[4] Anilkumar, K.K., Manoj, V.J. & Sagi, T.M. A review on computer aided detection and classification of leukemia. Multimed Tools Appl 83, 17961–17981 (2024). https://doi.org/10.1007/s11042-023-16228-6.

[5] Yadav, D.P., Kumar, D., Jalal, A.S. et al. Morphological diagnosis of hematologic malignancy using feature fusion-based deep convolutional neural network. Sci Rep 13, 16988 (2023). https://doi.org/10.1038/s41598-023-44210-7.

[6] Zhang L, Habeebu SSM, Li W. Prognostic and Predictive Biomarkers in Precursor B-cell Acute Lymphoblastic Leukemia. In: Li W, editor. Leukemia [Internet]. Brisbane (AU): Exon Publications; 2022 Oct 16. Chapter 10. Available from: https://www.ncbi.nlm.nih.gov/books/NBK586214/ doi: 10.36255/exon-publications-leukemia-biomarkers-lymphoblastic-leukemia.

[7] Samuel J. Pirruccello, Molly S. Bicak, Bruce G. Gordon, Kazimiera Gajl-Peczalska, David J. Gnarra, Peter F. Coccia, Acute lymphoblastic leukemia of NK-cell lineage: Responses to IL-2, Leukemia Research, Volume 13, Issue 9, 1989, Pages 735-743, ISSN 0145-2126, https://doi.org/10.1016/0145-2126(89)90086-6.

[8] Sedick Q, Alotaibi S, Alshieban S, Naheet KB, Elyamany G. Natural Killer Cell Lymphoblastic Leukaemia/Lymphoma: Case Report and Review of the Recent Literature. Case Rep Oncol. 2017 Jul 7;10(2):588-595. doi: 10.1159/000477843. PMID: 28868017; PMCID: PMC5567073.

[9] Das, P. K., & Meher, S. (2021). An efficient deep convolutional neural network based detection and classification of acute lymphoblastic leukemia. Expert Systems with Applications, 183, 115311. https://doi.org/10.1016/j.eswa.2021.115311.

[10] M. Tanveer, A. H. Rashid, M. Ganaie, M. Reza, I. Razzak, and K.L. Hua, "Classification of alzheimer's disease using ensemble of deep neural networks trained through transfer learning," IEEE J. Biomed. Health Informat., vol. 26, no. 4, pp. 1453–1463, Apr. 2022.

[11] Jha KK, Dutta HS. Nucleus and cytoplasm-based segmentation and actor-critic neural network for acute lymphocytic leukaemia detection in single cell blood smear images. Med Biol Eng Comput. 2020 Jan;58(1):171-186. doi: 10.1007/s11517-019-02071-1. Epub 2019 Dec 6. PMID: 31811554.

[12] Marzahl, C., Aubreville, M., Voigt, J., Maier, A. (2019). Classification of Leukemic B-Lymphoblast Cells from Blood Smear Microscopic Images with an Attention-Based Deep Learning Method and Advanced Augmentation Techniques. In: Gupta, A., Gupta, R. (eds) ISBI 2019 C-NMC Challenge: Classification in Cancer Cell Imaging. Lecture Notes in Bioengineering. Springer, Singapore. https://doi.org/10.1007/978-981-15-0798-4_2.

[13] Luis H.S. Vogado, Rodrigo M.S. Veras, Flavio. H.D. Araujo, Romuere R.V. Silva, Kelson R.T. Aires, Leukemia diagnosis in blood slides using transfer learning in CNNs and SVM for classification, Engineering Applications of Artificial Intelligence, Volume 72, 2018, Pages 415-422, ISSN 0952-1976, https://doi.org/10.1016/j.engappai.2018.04.024.

[14] Rezayi, S., Mohammadzadeh, N., Bouraghi, H., Saeedi, S., & Mohammadpour, A. (2021). Timely diagnosis of acute lymphoblastic leukemia using artificial intelligence-oriented deep learning methods. Computational Intelligence and Neuroscience, 2021, 1–12. https://doi.org/10.1155/2021/5478157.
[15] G. Atteia, A. Alhussan, and N. Samee, "BO-ALLCNN: Bayesian-based optimized CNN for acutely mphoblastic leukemia detection in microscopic blood smear images," Sensors, vol. 22, no. 15, p. 5520, Jul. 2022.
[16] Kulhalli, R., Savadikar, C., Garware, B. (2019). Toward Automated Classification of B-Acute Lymphoblastic Leukemia. In: Gupta, A., Gupta, R. (eds) ISBI 2019 C-NMC Challenge: Classification in Cancer Cell Imaging. Lecture Notes in Bioengineering. Springer, Singapore. https://doi.org/10.1007/978-981-15-0798-4_7.
[17] Park, S., Park, Y. H., Huh, J., Baik, S. M., & Park, D. J. (2024). Deep learning model for differentiating acute myeloid and lymphoblastic leukemia in peripheral blood cell images via myeloblast and lymphoblast classification. Digital Health, 10. https://doi.org/10.1177/20552076241258079.
[18] Bibi, N., Sikandar, M., Ud Din, I., Almogren, A., & Ali, S. (2020). IoMT-based automated detection and classification of leukemia using deep learning. Journal of Healthcare Engineering, 2020, 1–12. https://doi.org/10.1155/2020/6648574.
[19] Veeraiah N, Alotaibi Y, Subahi AF. MayGAN: Mayfly optimization with Generative Adversarial Network-based Deep Learning Method to classify leukemia form blood smear images. Comput Syst Sci Eng. 2023;46(2):2039–58.
[20] Wang, Q., Bi, S., Sun, M., Wang, Y., Wang, D., & Yang, S. (2019). Deep learning approach to peripheral leukocyte recognition. PloS One, 14(6), e0218808. https://doi.org/10.1371/journal.pone.0218808.
[21] Jawahar, Malathy, L. Jani Anbarasi, Sathiya Narayanan, and Amir H. Gandomi. "An attention-based deep learning for acute lymphoblastic leukemia classification." Scientific Reports 14, no. 1 (2024): 17447.
[22] Abbasi, Erum Yousef, Zhongliang Deng, Qasim Ali, Adil Khan, Asadullah Shaikh, Mana Saleh Al Reshan, Adel Sulaiman, and Hani Alshahrani. "A machine learning and deep learning-based integrated multi-omics technique for leukemia prediction." Heliyon 10, no. 3 (2024).
[23] E. Khosla and D. Ramesh, "Phase classification of chronic myeloid leukemia using convolution neural networks," 2018 4th International Conference on Recent Advances in Information Technology (RAIT), Dhanbad, India, 2018, pp. 1-6, doi: 10.1109/RAIT.2018.8389068.
[24] Rehman Amjad, Abbas Naveed, Saba Tanzila, Ijaz ur Rahman Syed, Mehmood Zahid, Kolivand Hoshang. Classification of Acute Lymphoblastic Leukaemia using deep learning. Microsc Res Tech 2018;81:1310–7. https://doi.org/10.1002/jemt.23139.
[25] Arivuselvam, B. and Sudha, S. 'Leukemia Classification Using the Deep Learning Method of CNN'. 1 Jan. 2022 : 567 – 585.
[26] https://www.kaggle.com/datasets/mehradaria/leukemia.
[27] Adleberg, Jason, et al. "Predicting patient demographics from chest radiographs with deep learning." Journal of the American College of Radiology 19.10 (2022): 1151-1161.
[28] Zhong, Haixin, and Rubin Wang. "A visual-degradation-inspired model with HSV color-encoding for contour detection." Journal of Neuroscience Methods 369 (2022): 109423.
[29] Ghaderzadeh M, Aria M, Asadi F. X-ray equipped with artificial intelligence: changing the COVID-19 diagnostic paradigm during the pandemic. Biomed Res Int. 2021:9942873. doi:10.1155/2021/9942873.
[30] Wei, Guoliang, et al. "An improved and random synthetic minority oversampling technique for imbalanced data." Knowledge-based systems 248 (2022): 108839.
[31] Chlap, Phillip, et al. "A review of medical image data augmentation techniques for deep learning applications." Journal of medical imaging and radiation oncology 65.5 (2021): 545-563.
[32] Cynthia, Eka Pandu, et al. "Convolutional Neural Network and Deep Learning Approach for Image Detection and Identification." Journal of Physics: Conference Series. Vol. 2394. No. 1. IOP Publishing, 2022.
[33] Awang, Mohd Khalid, et al. "Classification of Alzheimer disease using DenseNet-201 based on deep transfer learning technique." Plos one 19.9 (2024): e0304995.
[34] Wen, L., Li, X. & Gao, L. A transfer convolutional neural network for fault diagnosis based on ResNet-50. Neural Comput & Applic 32, 6111–6124 (2020). https://doi.org/10.1007/s00521-019-04097-w.
[35] Rajesh, B., and B. L. Muralidhara. "Image inpainting via generative multi-column with the aid of deep convolutional neural networks." Base University Working Papers 4 (2021): 425-426.

Research Article

[36] Ali, Yasser, Farrokh Janabi-Sharifi, and Soosan Beheshti. "Echocardiographic image segmentation using deep Res-U network." Biomedical Signal Processing and Control 64 (2021): 102248.
[37] Reddy, K. Shyam Sunder, et al. "An automated system for indian currency classification and detection using cnn." E3S Web of Conferences. Vol. 430. EDP Sciences, 2023.
[38] Eckle, Konstantin, and Johannes Schmidt-Hieber. "A comparison of deep networks with ReLU activation function and linear spline-type methods." Neural Networks 110 (2019): 232-242.
[39] Sandler, Mark, Andrew Howard, Menglong Zhu, Andrey Zhmoginov, and Liang-Chieh Chen, Mobilenetv2: Inverted residuals and linear bottlenecks," In Proceedings of the IEEE Conference on Computer Vision and Pattern Recognition, pp. 4510-4520. 2018.
[40] Nguyen, Hoanh. "Fast object detection framework based on mobilenetv2 architecture and enhanced feature pyramid." J. Theor. Appl. Inf. Technol 98.05 (2020): 812-824.
[41] Nguyen, Hoanh. "Fast object detection framework based on mobilenetv2 architecture and enhanced feature pyramid." J. Theor. Appl. Inf. Technol 98.05 (2020).
[42] Shah, Rajvi, et al. "Detection of different types of blood cells: A comparative analysis." 2022 IEEE international conference on distributed computing and electrical circuits and electronics (ICDCECE). IEEE, 2022.
[43] J. Tang, Q. Su, B. Su, S. Fong, W. Cao, and X. Gong, "Parallel ensemble learning of convolutional neural networks and local binary patterns for face recognition," Comput. Methods Programs Biomed., vol. 197, Dec. 2020, Art. no. 105622.
[44] Kulhalli, R., Savadikar, C., Garware, B. (2019). Toward Automated Classification of B-Acute Lymphoblastic Leukemia. In: Gupta, A., Gupta, R. (eds) ISBI 2019 C-NMC Challenge: Classification in Cancer Cell Imaging. Lecture Notes in Bioengineering. Springer, Singapore. https://doi.org/10.1007/978-981-15-0798-4_7.
[45] A. Genovese, M. S. Hosseini, V. Piuri, K. N. Plataniotis and F. Scotti, "Histopathological Transfer Learning for Acute Lymphoblastic Leukemia Detection," 2021 IEEE International Conference on Computational Intelligence and Virtual Environments for Measurement Systems and Applications (CIVEMSA), Hong Kong, China, 2021, pp. 1-6, doi: 10.1109/CIVEMSA52099.2021.9493677.
[46] D. R. Putri, A. Jamal, and A. A. Septiandri, "Acute lymphoblastic leukemia classification in nucleus microscopic images using convolutional neural networks and transfer learning," in Proc. 2nd Int. Conf. Artif. Intell. Data Sci. (AiDAS), Sep. 2021, pp. 1–6, doi: 10.1109/AiDAS53897.2021.9574176.
[47] Rezayi, S., Mohammadzadeh, N., Bouraghi, H., Saeedi, S., & Mohammadpour, A. (2021). Timely diagnosis of acute lymphoblastic leukemia using artificial intelligence-oriented deep learning methods. Computational Intelligence and Neuroscience, 2021, 1–12. https://doi.org/10.1155/2021/5478157.
[48] Park, S., Park, Y. H., Huh, J., Baik, S. M., & Park, D. J. (2024). Deep learning model for differentiating acute myeloid and lymphoblastic leukemia in peripheral blood cell images via myeloblast and lymphoblast classification. Digital Health, 10. https://doi.org/10.1177/20552076241258079.
[49] S. Rani B, G. B, S. G Shivaprasad Yadav, G. Shivakanth and M. B M, "Deep Learning Based Cancer Detection in Bone Marrow using Histopathological Images," 2023 IEEE International Conference on Integrated Circuits and Communication Systems (ICICACS), Raichur, India, 2023, pp. 1-8, doi: 10.1109/ICICACS57338.2023.10100116.